

EXTINCTION, THE ELEPHANT IN THE ROOM THAT HINDERS OPTICAL GALACTIC OBSERVATIONS

J. Maíz Apellániz¹

¹*Centro de Astrobiología, CSIC-INTA, campus ESAC.*

Camino bajo del castillo s/n, 28 692 Villanueva de la Cañada, Madrid, Spain.

Abstract. Extinction is the elephant in the room that almost everyone tries to avoid when analyzing optical/IR data: astronomers tend to find a quick fix for it that the referee will accept, but that does not mean such a solution is correct or even optimal. In this contribution I address three important issues related to extinction that are commonly ignored and present current and future solutions for them: [1] Extinction produces non-linear photometric effects, [2] the extinction law changes between sightlines, and [3] not all families of extinction laws have the same accuracy.

Key words: Dust, extinction — Galaxy: structure — Methods: data analysis — Methods: observational — Stars: early-type

1. Introduction

Interstellar extinction has been studied for almost a century and for a novice in the topic it may be surprising how much was already known about it at the early stages of that period. Trumpler (1934) describes extinction phenomena in terms of monochromatic (for single lines), selective (color excess) and general absorption (or proper extinction if one includes scattering), and as the existence of obscuration effects (dark areas of the sky devoid of visible stars). Baade & Minkowski (1937) and Morgan (1944) noticed that the extinction law towards Orion is peculiar, implying that a uniform extinction law does not exist for the whole sky. Stebbins & Whitford (1943) produced the first attempt to compute an extinction law as a function of wavelength.

The 1950s brought the advent of medium-scale (hundreds of stars) photoelectric *UBV* surveys of OB stars and, from them, the use of the *Q* parameter to measure their extinctions and estimate spectral types based on the behavior of the extinction law and the fact that the ratio of to-

tal to selective extinction $R_V \equiv A_V/E(B - V)$ is close to 3.0 for many sightlines (Johnson & Morgan 1953; Hiltner & Johnson 1956). At around the same time, Blanco (1956, 1957) recognized the existence of photometric bandwidth effects in the analysis of the photometry of those stars, leading to non-linear extinction trajectories in color-magnitude and color-color diagrams and, eventually, to the dependence of R_V not only on the type of dust but also on its amount as well as on the SED of the star. The following two decades saw a number of such optical extinction studies of OB stars using mostly the Johnson and Strömberg photometric systems.

The extension to other wavelength regimes started in the 1970s and took off with the launch of IUE in 1978 and the opening of moderately large ultraviolet samples and with the subsequent pioneering work of Rieke & Lebofsky (1985) in the infrared. Those led to the seminal work of Cardelli et al. (1989), the first family of UV-optical-IR extinction laws dependent on a parameter, the ratio of total to selective extinction, to determine both the amount and type of dust along the sightline.

The most recent development in extinction studies has taken place in the last quarter of a century with the appearance of large-scale photometric surveys, with sample increases of several orders of magnitude and the development of dedicated pipelines for the uniform processing of the data. In the NIR the most important step was the publication of 2MASS in 2003 (Skrutskie et al. 2006) and in the optical a number of surveys became available in the period such as SDSS (York et al. 2000) and IPHAS (Drew et al. 2005). The final step was the publication of the different *Gaia* data releases (Brown et al. 2016), with the availability of astrometry, (spectro)photometry, spectroscopy, and variability for $\sim 10^9$ stars. The combination of those surveys have brought us to a new era, both in terms of data volume and in the types of stars used to derive extinction, which are now of late type in most studies.

Why do I call extinction the elephant in the room? Because it is an obvious phenomenon in astronomy but it is undesired and most researchers want to just correct for it in a simple and quick way. The object of many papers is to obtain magnitudes and colors of astronomical objects and extinction is just a nuisance that gets in the way. Unfortunately, some of the simple and quick solutions ignore the complexities of the problem and lead to biased results. In this contribution I address the three main reasons why this happens:

1. **Extinction is a non-linear effect in magnitude or color.** In general, doubling the amount of dust does not double A_V or $E(B - V)$ and the same amount and type of dust does not produce the same A_V or of $E(B - V)$ in two stars with different SEDs. One needs to use monochromatic definitions for the amount and type of dust, so neither $E(B - V)$ nor R_V are appropriate. One should use their monochromatic equivalents, e.g. $E(4405 - 5495)$ and R_{5495} .
2. **The extinction law changes between sightlines.** R_{5495} is not the same everywhere. Many times it is within the canonical range of 3.0-3.2 but in a significant number of occasions it is outside that range (mostly > 3.2). R_{5495} is not even constant within a small region, especially if it includes diverse ISM environments such as H II regions. Furthermore, some measurements of R_{5495} use invalid or outdated approximations.
3. **No existing family of extinction laws accurately covers the UV-optical-IR range.** The two most commonly used, Cardelli et al. (1989) and Fitzpatrick (1999) can have significant photometric residuals already for stars with $E(4405 - 5495) \sim 1.0$. Maíz Apellániz et al. (2014) works well up to $E(4405 - 5495) \sim 2.0$ and does a reasonable job even around $E(4405 - 5495) \sim 3.0$ but does not extend to the UV and has the incorrect behavior in the IR.

In the next three sections I address each of those reasons and provide recipes when available. I end up analyzing prospects for the future.

2. Non-linearity of extinction

Extinction as a function of wavelength is defined as the ratio of the observed (extinguished) to the unextinguished spectral energy distributions (SEDs) expressed in magnitudes:

$$A(\lambda) = -2.5 \log_{10} \left(\frac{F_{\lambda}(\lambda)}{F_{\lambda,0}(\lambda)} \right). \quad (1)$$

The extinction in a given band such as V is the difference between the observed and the unextinguished magnitudes, which for a photon-counting detector such as a CCD can be expressed as:

$$A_V \equiv V - V_0 = -2.5 \log_{10} \left(\frac{\int P_V(\lambda) F_\lambda(\lambda) \lambda d\lambda}{\int P_V(\lambda) F_{\lambda,0}(\lambda) \lambda d\lambda} \right), \quad (2)$$

where $P_V(\lambda)$ is the sensitivity curve for the V band. In an equivalent manner, for the B band we have:

$$A_B \equiv B - B_0 = -2.5 \log_{10} \left(\frac{\int P_B(\lambda) F_\lambda(\lambda) \lambda d\lambda}{\int P_B(\lambda) F_{\lambda,0}(\lambda) \lambda d\lambda} \right). \quad (3)$$

To compute the values in Eqns 2 and 3 we need to substitute F_λ using Eqn. 1 and define $A(\lambda)$. The traditional (band-integrated) $B-V$ color excess is defined as the difference in extinction between the B and V bands:

$$E(B - V) \equiv A_B - A_V = (B - V) - (B - V)_0 \quad (4)$$

and the (band-integrated) ratio of total to selective extinction is defined as the ratio of Eqns. 2 and 4:

$$R_V \equiv \frac{A_V}{E(B - V)}. \quad (5)$$

The extinction law is simply the extinction normalized by some measurement of the amount of dust. This can be, for example, the value of $A(\lambda)$ at a given wavelength or the difference between $A(\lambda)$ at two different wavelengths. What should not be used as a normalization is a band-integrated extinction (such as those in Eqns. 2 or 3) or color excess (such as that in Eqn. 4). Why? **Because band-integrated quantities depend in a complex way on the SEDs.** In other words, A_V and $E(B - V)$ are not direct measurements of the amount of dust, as the same amount of dust on the sightline of a red and a blue star yield different values of A_V or $E(B - V)$. To show that, following Maíz Apellániz (2004) I use as the amount of dust $E(4405 - 5495)$, the monochromatic equivalent of $E(B - V)$, and apply the family of extinction laws of Maíz Apellániz et al. (2014)¹ to different SEDs from the library of Maíz Apellániz (2013b). Results are shown in Fig. 1, where it is clearly seen that the commonly used approximations of $E(B - V) \approx E(4405 - 5495)$ and $R_V \approx R_{5495}$ are only valid for hot stars with low extinction. Indeed, the reason why in Maíz Apellániz (2004) the

¹The result does not change substantially for other families, see Maíz Apellániz (2013a) for the equivalent plots using Cardelli et al. (1989).

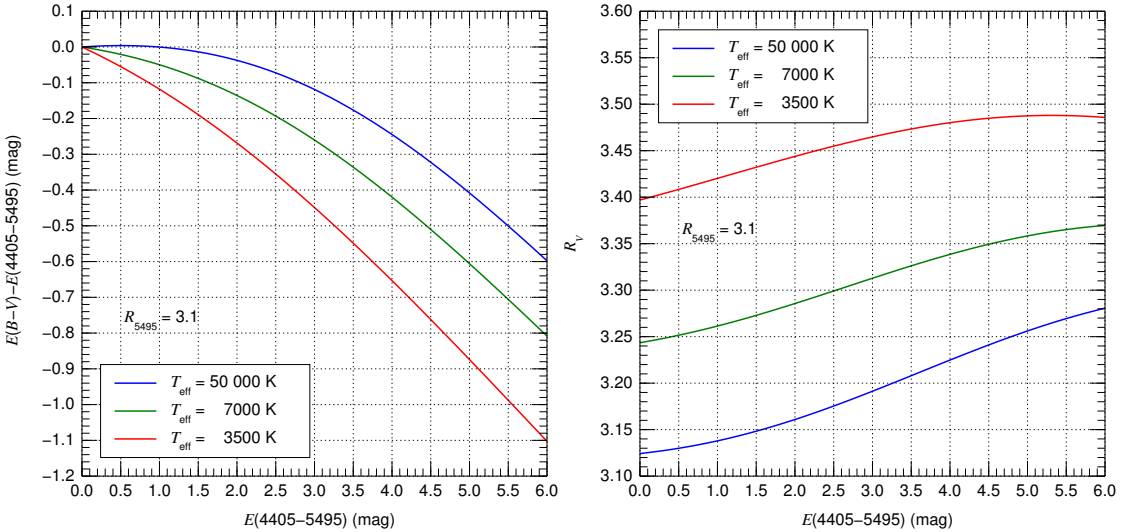


Figure 1: (left) $E(B-V) - E(4405 - 5495)$ and (right) R_V as a function of $E(4405 - 5495)$ for a Maíz Apellániz et al. (2014) extinction law with $R_{5495} = 3.1$ and three main-sequence stars with different T_{eff} . $E(B - V) \approx E(4405 - 5495)$ and $R_V \approx R_{5495}$ only for hot stars with low extinctions.

wavelengths of 4405 Å and 5495 Å were chosen as representative of B and V , respectively, was to allow for those approximations to be valid in that regime and, in that way, let the classic extinction measurements of OB stars remain approximately valid.

As I have previously mentioned, bandwidth effects in photometry were known already in the 1950s. However, there is no mention of them in Cardelli et al. (1989), where $E(B - V)$ is used as the amount of extinction and R_V as the type of extinction. Fitzpatrick (1999) mentions the difference between monochromatic and band-integrated quantities but he still uses $E(B - V)$ and R_V as parameters². For their samples the difference is small, as both papers use OB stars with low extinction (see below). Still, the formulae in those papers are inconsistent and need to be adapted to monochromatic quantities when implemented to allow them to be applied to SEDs of arbi-

²The latter is called simply R but its definition is that of R_V . Also, due to the different definitions of central wavelengths, if R is considered as the monochromatic definition for the extinction law, then it is not exactly R_{5495} .

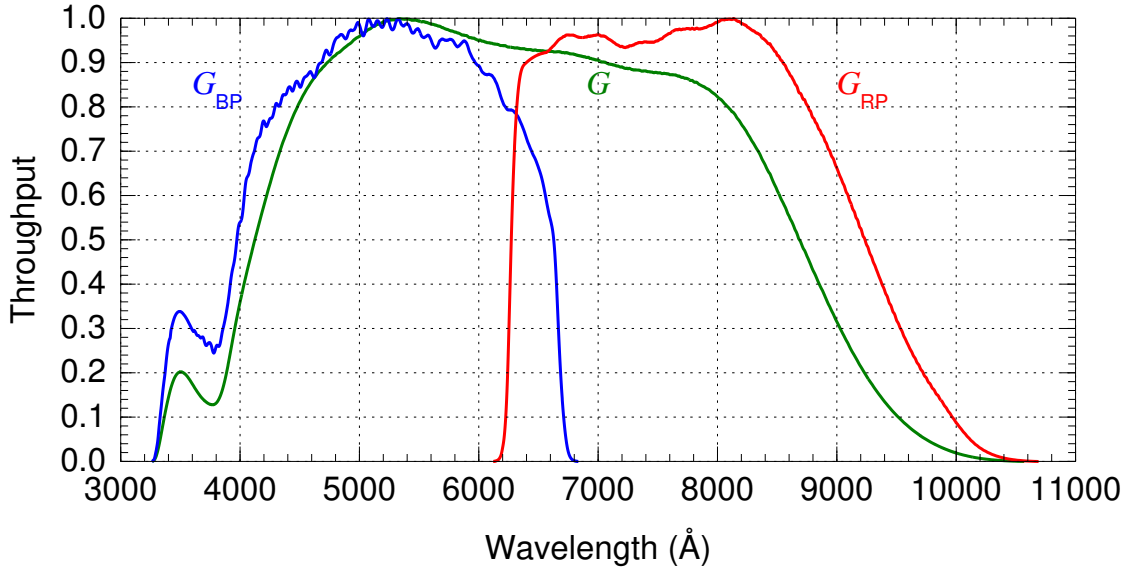


Figure 2: Throughputs for the *Gaia* EDR3 $G+G_{BP}+G_{RP}$ photometric system (Weiler et al. in prep.).

rary temperatures and extinctions.

Despite claims to the contrary, bandwidth effects are always present. If they have been ignored in the past it may have been because samples were more restricted in temperature and extinction and because past photometric calibrations were not as accurate as current ones (see Maíz Apellániz 2005, 2006, 2007 for examples). Having said that, non-linearity starts becoming noticeable at lower extinctions for broader filters than for narrower ones (e.g. Johnson vs. Strömgren) and for wavelength regions where the extinction law is steeper. Those conditions make non-linearity a stronger effect for the *Gaia* $G+G_{BP}+G_{RP}$ system than for other optical photometric systems, as the G band is very broad (Fig. 2) and the photometric calibration of *Gaia* is better than that of any optical ground-based system (Maíz Apellániz & Weiler 2018).

Gaia data processing correctly differentiates between monochromatic and band-integrated quantities. For example, Apsis (Creevey et al. 2023) provides one monochromatic extinction (A_0 , with the wavelength being 5414 Å), three band-integrated extinctions (A_G , A_{BP} , and A_{RP}), and one

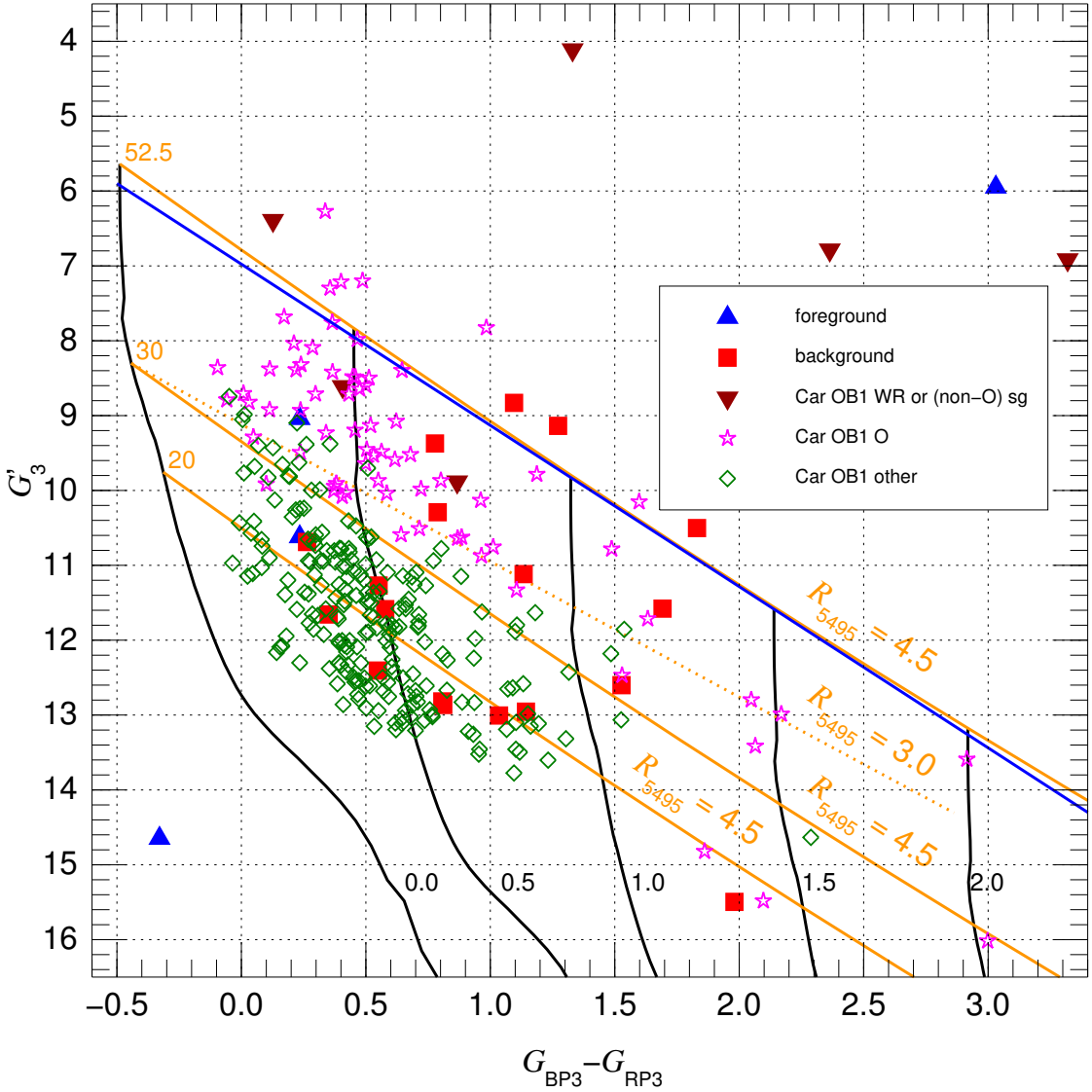


Figure 3: Gaia EDR3 Carina OB1 CMD adapted from Berlanas et al. (2023). The orange lines show extinction tracks for MS stars of different T_{eff} (indicated in kK at their left ends) and R_{5495} (also labelled). For the 52.5 kK extinction track with $R_{5495} = 4.5$ I have also drawn a blue straight line next to it to show the curvature effect.

band-integrated color excess or reddening $[E(G_{\text{BP}} - G_{\text{RP}})]$, each one adequately identified. Non-linearity appears both in *Gaia* CMDs and color-color diagrams. A sample CMD is shown in Fig. 3, adapted from the analysis of Carina OB1 by Berlanas et al. (2023). The extinction tracks are shown in orange and computed for different T_{eff} and R_{5495} values using the family of Maíz Apellániz et al. (2014). As the vertical scale comprises 13 magnitudes, the curvature is not apparent at first but plotting a straight line next to one of them (in blue) shows that the effect amounts to several tenths of a magnitude over the extinction range plotted in this case (most stars that appear in the plot are blue MS stars that have been displaced towards the lower right corner by the strong differential extinction in the region). A sample color-color diagram is shown in Fig. 4, as it appeared in Maíz Apellániz & Weiler (2018). The stellar locus is highly curved due to extinction and the different values of T_{eff} , with both effects being relatively similar due to the *Gaia* filter design, and follows the result of the throughputs in that paper (labelled as MAW) with $R_{5495} = 3.0$ quite well (the extension towards the upper left part of the diagram is caused mostly by stars with contaminated photometry due to crowding or nebulosity).

In the NIR, extinction is smaller than in the optical for the same dust column but, at the same time, we can reach higher extinction values and non-linear effects appear sooner or later. As discussed in Maíz Apellániz et al. (2020), if non-linearity is ignored in IR studies, extinction measurement can be compromised. Some papers, such as Stead & Hoare (2009); Wang & Chen (2019); Nogueras-Lara et al. (2021) correctly deal with it but others do not. I show this in Fig. 5, which is taken from the Appendix in Maíz Apellániz et al. (2020). As we increase A_1 , the monochromatic extinction at $1 \mu\text{m}$, the color excess $E(J - H)$ clearly deviates from a non-linear behavior. The effect is stronger for higher values of α , the exponent in the assumed power-law NIR extinction. As we will see later, the current preferred value is $\alpha \sim 2.2$, so the effect is easy to notice already at relative lower values of A_1 .

As a summary of this section, extinction has a clear non-linear behavior in CMDs and color-color diagrams. The corollary is that one should not apply the commonly used approximation of defining a central wavelength for a filter and extinguish the photometry assuming that only the extinction law at that point is relevant. Extinction should be calculated using integrals such as Eqns. 2 and 3. As that may be computationally too expen-

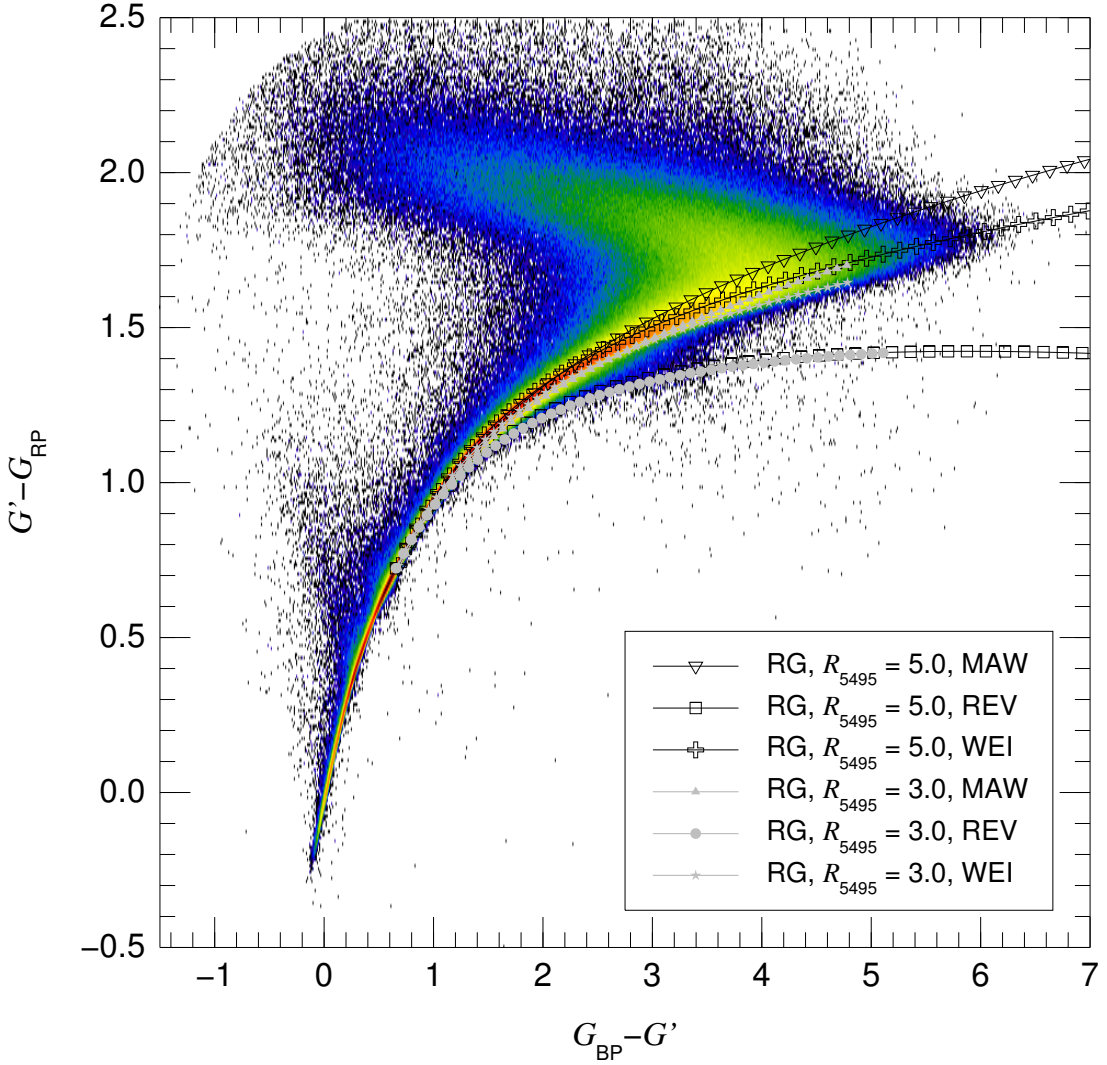


Figure 4: Gaia DR2 color-color diagram from Maíz Apellániz & Weiler (2018). The lines show the extinction tracks for red-clump stars with different assumptions about R_{5495} and the filter throughputs (the purpose of that paper was to identify those), with the associated symbols plotted at intervals of $E(4405 - 5495)$ of 0.1 mag.

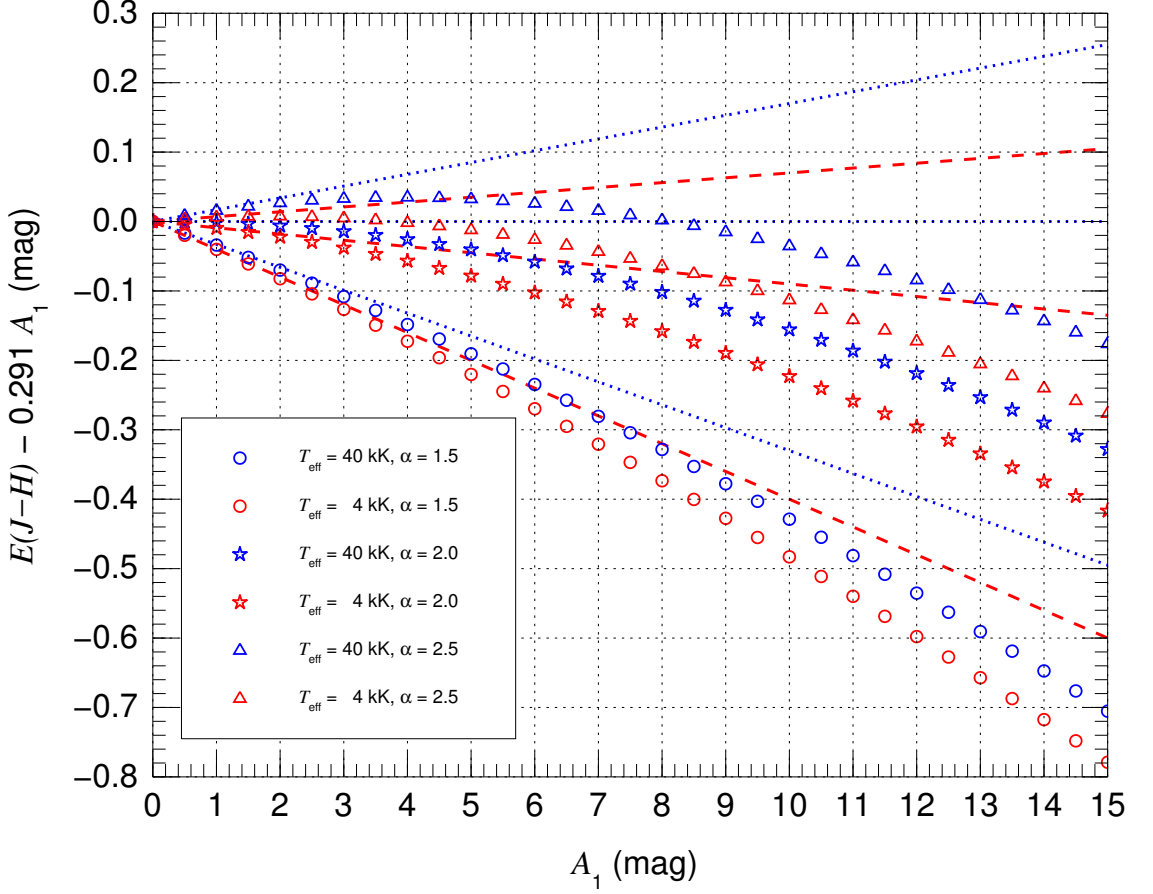


Figure 5: Band-integrated $E(J - H)$ color excess as a function of the monochromatic amount of extinction A_1 from Maíz Apellániz et al. (2020). Two effective T_{eff} (4 kK and 40 kK) and three values of the NIR slope α (1.5, 2.0, and 2.5) are used. Symbols are used for the actual values and lines for the extrapolation from the low-extinction regime.

sive when dealing with large samples and fitting procedures, one alternative is to compute a grid for the desired values of the extinction and interpolate with splines within the grid. This is the approach used by CHORIZOS (Maíz Apellániz 2004).

3. Variability of the extinction law

3.1. INTRODUCTION

As I mentioned in the introduction, the variability of the extinction law in the optical/IR has been known since the 1930s but it was not until the 1980s that the much stronger variability in the UV was discovered with IUE. Seaton (1979) produced an average UV extinction law from OAO-2, Copernicus, and TD-1 data but subsequent work revealed variability among Galactic sightlines (Hecht et al. 1982; Massa et al. 1983; Cardelli & Savage 1988) and between those and LMC (Howarth 1983; Fitzpatrick & Savage 1984; Clayton & Martin 1985; Fitzpatrick 1985, 1986) and SMC (Rocca-Volmerange et al. 1981; Lequeux et al. 1982; Prévot et al. 1984; Gordon & Clayton 1998; Maíz Apellániz & Rubio 2012) sightlines.

The studies of extinction of the 1980s culminated in the work of Cardelli et al. (1989), who, as previously mentioned, produced the first R_{5495} -dependent family of extinction laws. That family has a uniform behavior in the IR (based on Rieke & Lebofsky 1985) and a highly variable dependence on R_{5495} as a single parameter in the optical and UV. Another commonly used family of extinction laws, that of Fitzpatrick (1999), appeared a decade later and has a similar behavior to the Cardelli et al. (1989) one: non-variable in the IR and dependent on an R -like parameter in the optical and UV. In the next section I analyze their similarities and differences in more detail. I also address extinction-law variability in the IR later on. For the time being, I just point out that, given the range of extinctions covered by the previously mentioned two families of extinction laws, such IR extinction variability would have been very difficult to measure with the data available in the 1980s and 1990s.

3.2. METHODOLOGY

Before addressing the variability of the extinction law, I need to discuss how the extinction law and extinction in general are measured. In principle, $A(\lambda)$ is determined by Eqn. 1, so what we need is the observed SED determined from spectrophotometry, divide it by the unextinguished SED, obtain the logarithm, and multiply the result by -2.5 . As expected, that is more easily said than done for two reasons: [1] We do not know a priori

the unextinguished SED and [2] in most cases we do not have spectrophotometric data but only photometry. I address those two issues starting with the first one.

The unextinguished SED. The traditional method used, for example, in most of the 1980s work with IUE data, is called the pair method. One obtains the spectrum of an identical star with no extinction and uses it as a reference or standard for the unextinguished SED. The three problems associated with the pair method are: obtaining the ratio of the distances needed to normalize the fluxes, determining that the two stars are indeed identical, and finding the reference star itself. Of those, the third one is the most difficult one: OB stars are concentrated in the plane of the Milky Way and are usually at considerably distances, so extinction is almost never negligible (Maíz Apellániz & Barbá 2018). Due to those problems, in the last two decades most works have shifted towards using synthetic SEDs as a reference instead of observed ones (Maíz Apellániz 2004; Fitzpatrick & Massa 2005). For this alternative method we still have the first problem (flux normalization due to distance) and the last two are substituted by another two: making sure that the grid of synthetic SEDs is spectrophotometrically accurate and determining the parameters of the star (T_{eff} being the most important one but also $\log g$ and metallicity in some cases) to select the specific SED in the grid. I discuss these issues below.

Photometry instead of spectrophotometry. Analyses of UV extinction using IUE data in the 1980s had access to spectrophotometry in the ultraviolet but even those complemented the optical and IR ranges with photometry. As most current works use large-scale photometric optical/IR surveys as their data source for extinction determinations, photometry has become the most popular method to determine extinctions. Photometry has the advantage of large sample sizes but introduces problems with calibration for both the analyzed stars and for the standard system (see below) and only samples the extinction law at a coarse wavelength grid which then needs to be interpolated or modelled.

There are actually two related problems we are dealing with. One is determining the family of extinction laws that applies to an astrophysical regime (such as a given galaxy or environment) and another one calculating the extinction for a set of stars. In this section I start with the second problem, which assumes we already know the family of extinction laws, and in the next section I will address the more complex problem of determining the

family of extinction laws. To determine the extinction parameters (amount and type) we need to fit the observed photometry to the synthetic photometry derived from the SED models. Using χ^2 minimization, the problem can be expressed with these three equations:

$$\chi_{\text{red}}^2 = \frac{1}{N - \text{DoF}} = \sum_{i=1}^N \frac{(m_{i,\text{obs}} - m_{i,\text{syn}})^2}{\sigma_{i,\text{obs}}^2} \sim 1 \quad (6)$$

$$m_{i,\text{syn}} = -2.5 \log_{10} \left(\frac{\int P_i(\lambda) F_\lambda(\lambda) \lambda d\lambda}{\int P_i(\lambda) F_{\lambda,r}(\lambda) \lambda d\lambda} \right) + \text{ZP}_{i,r} \quad (7)$$

$$F_\lambda(\lambda) = F_{\lambda,0}(\lambda) e^{-0.4 A(\lambda)} \quad (8)$$

with the following definitions:

- χ_{red}^2 : Goodness of fit (reduced chi square).
- N : Number of filters/passbands.
- DoF: Degrees of freedom of fit (number of parameters).
- $m_{i,\text{obs}}$: Observed magnitude for filter/passband i .
- $m_{i,\text{syn}}$: Synthetic magnitude for filter/passband i .
- $\sigma_{i,\text{obs}}$: Observed magnitude uncertainty for filter/passband i .
- $P_i(\lambda)$: Sensitivity curve/throughput for filter/passband i .
- $F_\lambda(\lambda)$: Observed SED.
- $F_{\lambda,r}(\lambda)$: Reference system SED ($r = \text{Vega, ABmag, STmag}$).
- $\text{ZP}_{i,r}$: Photometric zero point for filter i in the reference system r .
- $F_{\lambda,0}(\lambda)$: Unextinguished SED.
- $A(\lambda)$: Extinction as a function of λ in mag.

The logical procedure is to generate an extinguished grid of SEDs using Eqn. 8 as a function of intrinsic (such as T_{eff} and $\log g$ or luminosity class) and extrinsic (such as amount and type of dust) parameters, including distance if it is not independently determined. The extinguished SED grid is transformed into an extinguished magnitude grid using Eqn. 7 and the parameters and their uncertainties are obtained through the fitting process

that uses Eqn. 6. This is the procedure used in CHORIZOS (Maíz Apellániz 2004) and in other equivalent codes. However, the devil is in the details and there are five different aspects that have to be considered. I describe them here, each color-coded in Eqns. 6 to 8 above.

Photometric calibration. There are three related aspects of photometric calibration to be considered: the absence of biases in the observed magnitudes, the proper estimation of the photometric uncertainties, and the correct characterization of the sensitivity curves. As already mentioned, old-style ground-based systems such as Johnson and Strömgren have problems inherent with the small samples analyzed by each author and with the presence of inconsistencies among different authors, leading to relatively large realistic uncertainties (Maíz Apellániz 2006, 2007). *Gaia* photometry, on the other hand, has the opposite problem: the large sample and consistent reduction leads to calibrations that are so accurate that small systematic effects can be detected, thus leading to improvements in the calibration itself (Maíz Apellániz & Weiler 2018). In this respect, it is important to distinguish that there are two types of photometric uncertainties. Internal uncertainties are those that do not make a comparison with an external system and, as such, are appropriate for variability studies such as in Maíz Apellániz et al. (2023). However, if we want to compare our observed magnitudes with synthetic ones, we also have to include the uncertainties in the knowledge of the photometric system (external uncertainties). The easiest thing to do is to use a calculated minimum uncertainty or to add a systematic uncertainty in quadrature to the observed one (Maíz Apellániz & Weiler 2018). If this is not done, chances are that we will have problems in our final check (see below). A similar issue can appear if our source is intrinsically variable and our photometry is obtained in different epochs, which is why a check for source variability is convenient (Maíz Apellániz et al. 2023).

Standard calibration. Photometric systems are calibrated with a reference SED that can be an astrophysical source such as Vega (Vega system) or a simple function such as in the ABmag or STmag systems (see e.g. Laidler et al. 2005). In the case of an astrophysical source, it needs to be determined independently (Bohlin & Gilliland 2004; Bohlin 2007, 2014). In all cases, the photometric zero point (in some references, called the differential zero point) needs to be calculated. It is a quantity that is supposed to be close to zero but seldom is actually zero due to the way photometric

surveys are calibrated (see Maíz Apellániz 2007; Maíz Apellániz & Weiler 2018 and references therein).

Model SEDs. Nowadays there are a number of choices for SED grids for stellar atmospheres of different characteristics. However, before using them one needs to read the fine print, as some are optimized to accurately describe stellar lines but not so much the absolute fluxes or have a detailed analysis in just some wavelength regions. One way to test them is to compare the derived synthetic photometry derived with the observed magnitudes of low-extinction stars. As an example, CHORIZOS uses a tailored SED grid built from different sources (Maíz Apellániz 2013b). For hot stars, the SEDs are mostly from TLUSTY (Lanz & Hubeny 2003, 2007) and accurately represent the optical colors of O and B stars. However, the NIR synthetic colors derived from TLUSTY are incorrect, so for long wavelengths the Munari et al. (2005) grid is used instead. Also, one should always check whether the grid includes the type of system we are observing: stars with emission lines or IR excesses and binary systems with components of very different T_{eff} will usually need to be analyzed with an SED grid with additional parameters.

Extinction. The main issue here is extinguishing the model SEDs (Eqn. 8) before integrating in wavelength (Eqn. 7) to correctly account for non-linear photometric effects, as discussed in the previous section. Furthermore, some papers use simple linear approximations to determine the amount and type of extinction from color-color relations: those determinations of $E(B - V)$ and R_V should be distrusted in general (and, once again, one should use monochromatic quantities for the amount and type of extinction, not band-integrated ones).

Final check. The last step to perform is to verify the goodness of the fit. Fitting a functional form to a data set and obtaining a result does not mean that the result makes sense: a straight line can be fit to data extracted from a parabola to derive a slope and an intercept but that does not mean that those two quantities accurately describe the data. Unfortunately, this step is omitted in many papers and one is left to wonder whether the results make sense or not. Going over the four previous aspects, if the fit is not as good as it should it could be due to a number of reasons: [1] The observed magnitudes may have systematic effects, their random uncertainties may be underestimated, or the sensitivity curve may not be properly characterized. [2] The photometric zero points may be incorrect. [3] The model SEDs may not properly represent the object. [4] The extinction law

may be incorrect. Any of these reasons may apply in different situations. Sometimes the problems will be in the calibration, in others we may have an interesting astrophysical case, such a star with a previously undetected IR excess. One way to understand what is going on is to analyze the fit residuals, as those may point out to e.g. systematic effects as a function of the amount of extinction, a telltale sign of issues with the extinction law (see Maíz Apellániz et al. 2014 for an example).

3.3. RESULTS

In Maíz Apellániz & Barbá (2018) we used the method described above to derive $E(4405 - 5495)$ and R_{5495} for 562 Galactic O stars. In a subsequent paper (Maíz Apellániz et al. 2021b), we selected a subsample of those and added some OB stars with notoriously high $E(4405 - 5495)$ or R_{5495} to obtain a golden sample of 120 OBA stars with measurements not only of those extinction properties but also of interstellar K I and C₂. We also detected a very broad interstellar absorption band of unknown origin centered around 7700 Å that should be incorporated into future families of extinction laws.

The results for the golden sample are shown in Fig. 6 and are derived from a combination of NIR (mostly 2MASS) and optical photometry (*Gaia*, Tycho-2, Johnson, and Strömgren). In general, it is difficult to determine R_{5495} from optical photometry alone, as the information encoded at longer wavelengths is needed to determine A_{5495} . The most important result from Fig. 6 is that there is a large scatter in the Galactic R_{5495} values: from a floor around 2.6 to values higher than 6.0. A similar range (3.1-6.7) was found for the 30 Dor sample in Maíz Apellániz et al. (2014) using HST photometry. The distributions in R_{5495} and $E(4405 - 5495)$ are not independent: the scatter in R_{5495} decreases as $E(4405 - 5495)$ increases and, in the limit of high extinction, most R_{5495} values concentrate in the 2.8-3.2 range. Therefore, the canonical values of 3.0-3.2 are still valid, but only as an approximation in that circumstance.

It is important to understand the uncertainties associated with both $E(4405 - 5495)$ and R_{5495} . Parameter uncertainties in CHORIZOS are calculated by properly sampling the multi-parameter space around the minimum χ^2 location, thus allowing for a correct characterization of their correlations (Maíz Apellániz 2004). In general, $E(4405 - 5495)$ can be deter-

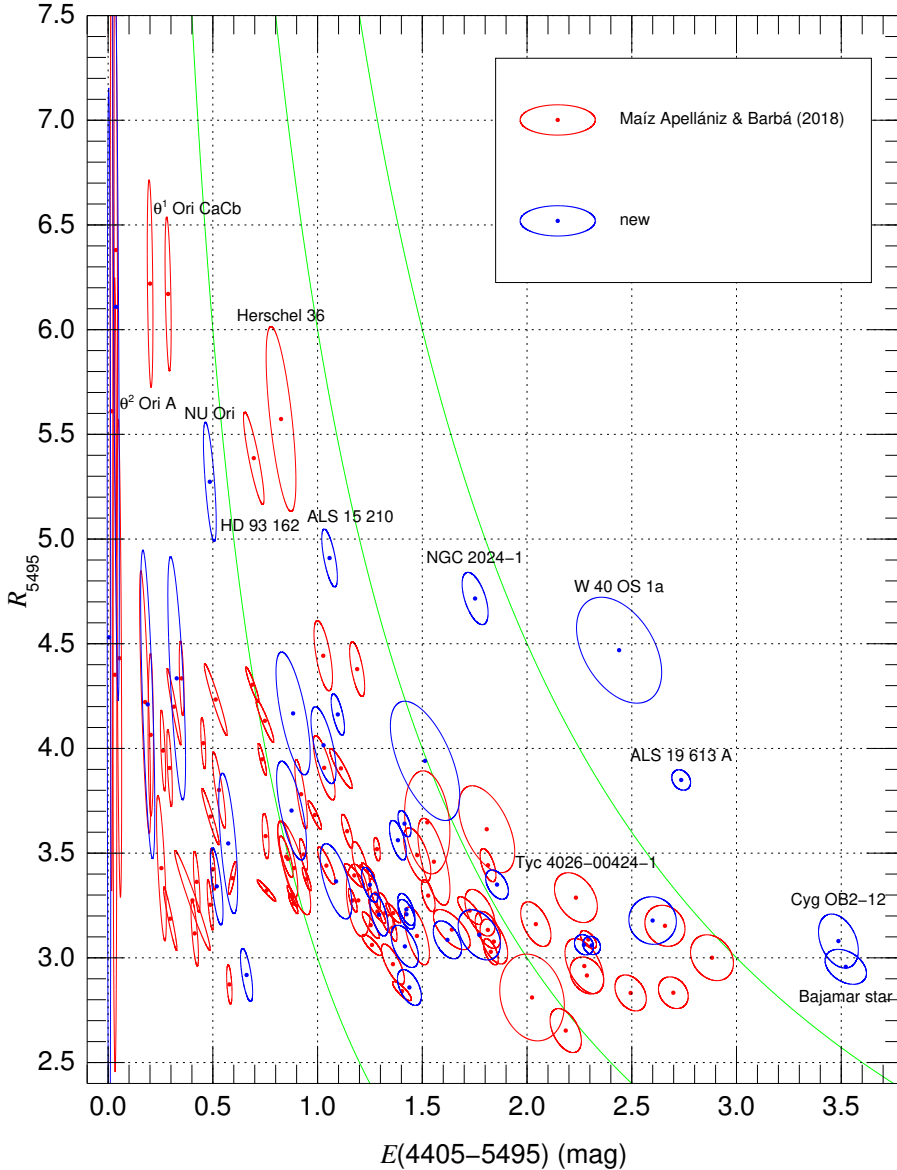


Figure 6: R_{5495} as a function of $E(4405 - 5495)$ for the sample of 120 OBA stars in Maíz Apellániz et al. (2021b). The color coding indicates whether the data appeared in Maíz Apellániz & Barbá (2018) or not. Green lines correspond (from left to right) to the values of A_{5495} of 3, 6, and 9 mag.

EXTINCTION, THE ELEPHANT IN THE ROOM

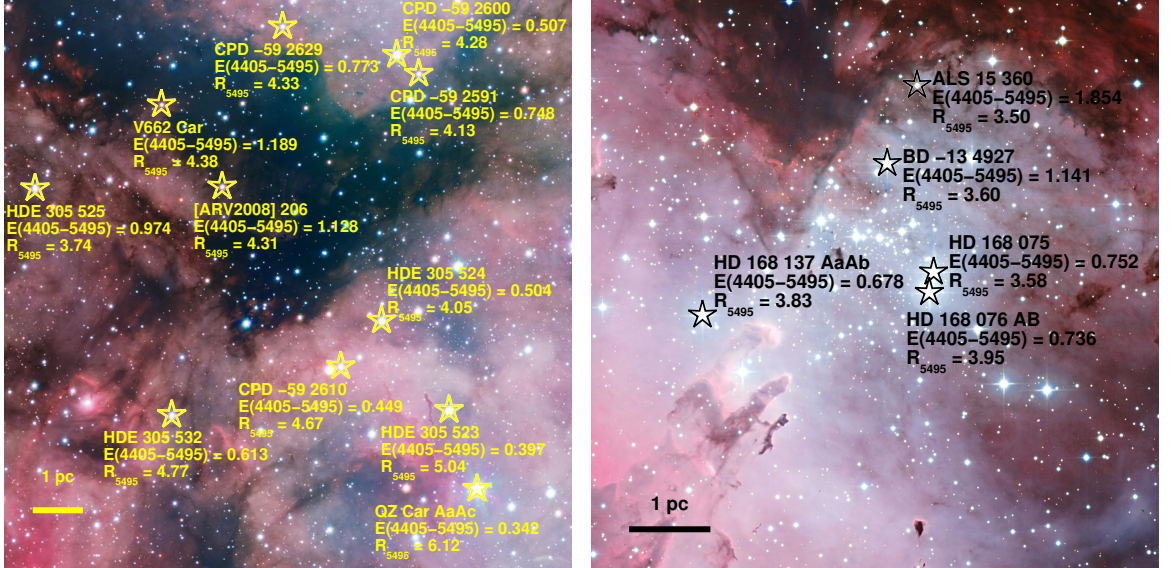


Figure 7: Extinction measurements for O stars in two H II regions: (left) the Carina Nebula and (right) M 16/NGC 6611. The two images are from ESO press releases 1250 ($BgrH\alpha$) and 0926 (BVR), respectively. North is towards the top and east towards the left and the approximate physical scale is indicated. Only a section of each H II region is shown to better visualize the dust lanes.

mined reasonably well (uncertainties of ~ 0.02 mag) at most extinctions as long as there is good-quality photometry. This is easy to understand as the intrinsic $(B - V)$ of OB stars $(B - V)_0$ is well determined and, to a first approximation, $E(4405 - 5495) \sim E(B - V)$ (but see Fig. 1) and from Eqn. 4 the uncertainties arise only from those in the measured (Johnson) $B - V$, which are of the order of 0.02 mag (see Table 9 in Maíz Apellániz 2006 and remember the previous point about realistic external photometric uncertainties)³. The uncertainties on R_{5495} , on the other hand, are much larger for small values of $E(4405 - 5495)$ than for large ones. The explanation is that R_{5495} is a measurement of the type of extinction and in the limit of low extinction information about it is limited. Interestingly, the sampling of χ^2 in the multi-parameter space shows that in most cases the uncertain-

³This is just a simplified version of what the code does and assumes that Johnson BV photometry is available. In reality, all used magnitudes contribute in some degree to the determination of $E(4405 - 5495)$.

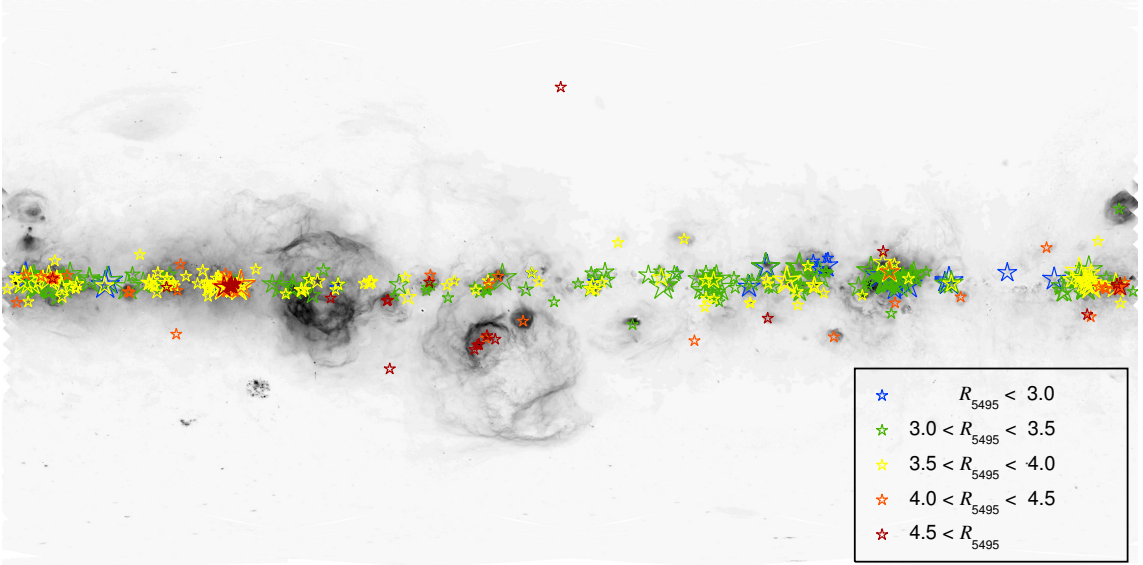


Figure 8: Extinction measurements for Galactic O stars plotted on top of the full-sky H α image of Finkbeiner (2003). Different colors are used for five ranges of R_{5495} with the size of the symbol increasing with $E(4405 - 5495)$. The background image is showed in a logarithmic intensity scale and in Galactic coordinates with a Cartesian projection centered on the Galactic anticenter.

ties in $E(4405 - 5495)$ and R_{5495} are anticorrelated: this is seen in Fig. 6 by the elongation of the ellipse uncertainties along the lines of constant A_{5495} . Therefore, the relative uncertainty of A_{5495} can be lower than those of both $E(4405 - 5495)$ and R_{5495} , something that is impossible in the absence of an anticorrelation. In other words, a method that properly measures extinction combining optical and NIR photometry can arrive at a more precise determination of A_{5495} (and hence, of A_V) than of either $E(4405 - 5495)$ or R_{5495} .

Where does the variability in the extinction law originate? Already Baade & Minkowski (1937) pointed out that the high values of R_{5495} in Orion are likely due to a larger than average grain size for the dust particles, a view that has remained since then. In Maíz Apellániz & Barbá (2018) we reviewed the literature and presented results showing how H II regions have large internal variability in R_{5495} and $E(4405 - 5495)$, with regions with intense nebular emission typically having high R_{5495} and low

$E(4405 - 5495)$ and regions close to or on top of dust lanes having low R_{5495} and high $E(4405 - 5495)$ (Fig. 7). In addition, a map of the R_{5495} measurements in Maíz Apellániz & Barbá (2018) over the whole sky (Fig. 8) shows that high-latitude stars, which are relatively nearby and for which the Local Bubble contribution should be larger than average, tend to have high values of R_{5495} . This led us in Maíz Apellániz & Barbá (2018) to propose a scenario in which there are three different ISM regimes depending on the ambient UV radiation level:

- Regions with intense UV radiation have large values of R_{5495} (> 4). This includes H II regions but also cavities filled with hot gas (e.g. the Local Bubble) where UV radiation can travel for long distances.
- Regions with low intensity of UV radiation have small values of R_{5495} (< 3). These regions are those with significant column densities of CO or those that are easily detected as dust lanes in the optical.
- Regions with intermediate levels of UV radiation have values of R_{5495} between 3 and 4. These regions represent a typical warm to cold ISM (excluding H II regions, cavities, and molecular clouds) that fills the majority of the volume in the Galactic disk.

Therefore, high levels of UV radiation correspond to large average grain sizes (high R_{5495}). The likely explanation is that ISM regions with large values of R_{5495} are produced by the selective destruction of smaller dust grains with respect to large grains. Such a selective destruction could be caused by thermal sputtering (Draine 2011) or heating by EUV radiation (Guhathakurta & Draine 1989; Jones 2004).

3.4. A COMPARISON WITH GAIA DR3 RESULTS

To see the importance of including R_{5495} in an analysis of extinction, here I compare the results from Maíz Apellániz et al. (2021b) with the *Gaia* DR3 results of Creevey et al. (2023). That paper presents the *Gaia*-DPAC analysis using the Astrophysical parameters inference system (Apsis). With a variety of information from different *Gaia* sources, they derive stellar and extinction parameters for a large sample of stars. Here I concentrate on the results from the ESP-HS module, the Extended Stellar

EXTINCTION, THE ELEPHANT IN THE ROOM

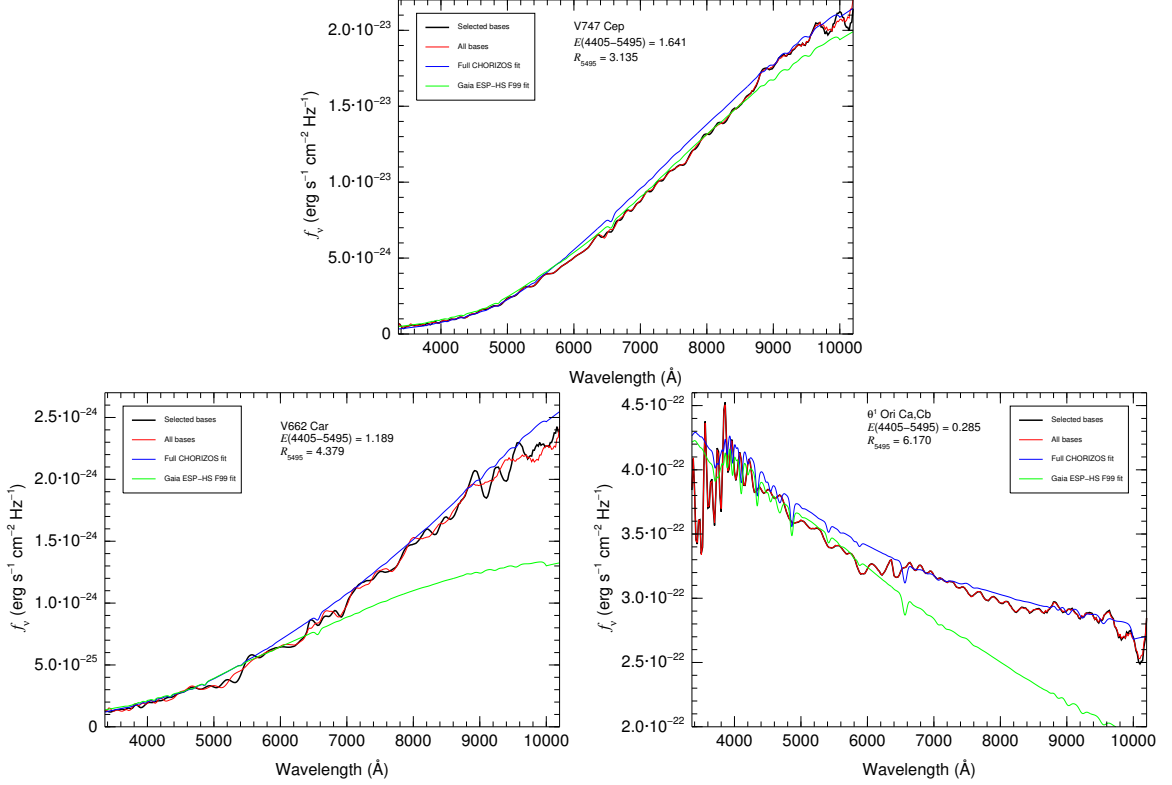


Figure 9: Comparison between the CHORIZOS results of Maíz Apellániz et al. (2021b) and the *Gaia* XP results of Creevey et al. (2023). The black/red lines are the input XP spectra using two choices of basis functions (to showcase the uncertainty in flux), the blue line is the SED derived from the CHORIZOS fit, and the green line the SED derived from the Creevey et al. (2023) XP fit (displaced to fit as much of the XP spectra as possible). The names of the stars and their CHORIZOS-derived values of $E(4405 - 5495)$ and R_{5495} are given in each panel, with the three stars selected to showcase different values of R_{5495} .

Parametrizer for Hot Stars, as that is the module which is more appropriate (and favorable) to use against the OBA-star analysis with CHORIZOS in Maíz Apellániz et al. (2021b).

The ESP-HS module uses a library of hot-star atmospheres to derive T_{eff} , $\log g$, A_0 (the equivalent to A_{5495} , see above), and d based on the parallax and the XP spectra (plus the RVS spectra for some stars). It fixes the equivalent of R_{5495} to 3.1 using the family of extinction laws of Fitzpatrick (1999). As a comparison, the analysis of Maíz Apellániz et al. (2021b) is based on photometric data (including *Gaia* and 2MASS) and fits $E(4405 - 5495)$,

R_{5495} , and $\log d$, fixing T_{eff} and the luminosity class (a proxy for $\log g$) from the spectral types, and using the family of extinction laws of Maíz Apellániz et al. (2014). I compare the results from the two procedures for three stars of different R_{5495} in Fig. 9.

The predicted CHORIZOS SED is a reasonable fit for the XP spectra of the three stars despite having been obtained prior to *Gaia* DR3. There are some small differences, both at small and large wavelength scales, some of which may be due to small deficiencies in the Maíz Apellániz et al. (2014) family of extinction laws and some due to systematic biases in the XP spectra. Among the first, I note that for V747 Cep there is a hint of the 7700 Å bump and for V662 Car there is a clear detection. Among the second, many of the wiggles seen are likely artifacts due to the extraction procedure as a series of basis functions (Carrasco et al. 2021).

As for the Creevey et al. (2023) results, the fit is reasonably good for V747 Cep, which has an R_{5495} of 3.135 ± 0.078 that is compatible with the assumed value of 3.1. On the other hand, the fit is bad for either V662 Car and θ^1 Ori Ca,Cb, which have values of R_{5495} significantly different from the assumed 3.1. The discrepancy is a natural consequence of the CHORIZOS fit being a good one, as there is no stellar SED of any T_{eff} with $R_{5495} = 3.1$ that resembles that of an O star with values of $R_{5495} > 4.0$ and a minimum amount of extinction. In other words, the Creevey et al. (2023) results are inconsistent with their own input data because they did not include the real solution among the set of possible ones, an example of “fitting a straight line to a parabola” (see above).

The conclusion of this analysis is that the parameters derived by assuming that R_{5495} is 3.1 everywhere are bound to fail in the cases where R_{5495} is significantly different and those cases, at least for OBA stars, are relatively common (Fig. 6). As an example, the ESP-HS analysis of V662 Car derives a value of $A_0 = 3.639 \pm 0.042$ mag. The equivalent A_{5495} calculated from CHORIZOS is 5.206 ± 0.038 mag, significantly higher. Another lesson is that NIR data need to be added to optical (spectro)photometry to correctly fit both the type and amount of extinction: Creevey et al. (2023) could not include 2MASS photometry in their analysis due to the DPAC policy of excluding non-*Gaia* data.

4. Families of extinction laws

4.1. HISTORY

As already mentioned, Cardelli et al. (1989) or CCM published the first family of extinction laws with a parameter describing the type of extinction (R_V though it should have been a monochromatic quantity such as R_{5495}) to add to the amount of extinction [$E(B - V)$ though it should have been a monochromatic quantity such as $E(4405 - 5495)$]. It was based on *UBVRIJHKL* photometry for the optical+IR part and IUE spectrophotometry for the UV part, thus covering the range from 1250 Å to 3.5 μm. As with most 1980s extinction papers, CCM is a UV-centric work, as the access to that range provided by IUE was the novelty at that time and that was where most of the interesting information was available. As it turned out, most papers that ended up using the family of extinction laws eventually applied it to the optical+IR ranges instead of to the ultraviolet, especially after the first decade⁴.

The CCM family is based on 29 low-extinction Galactic sightlines, of which only three have listed values with $E(B - V) > 1.0$ mag and even for those they are only 1.09 mag, 1.11 mag, and 1.22 mag. The listed covered range in R_V is 2.6-5.3. The reasons for those limitations are easy to understand: as an UV-centric study, objects with higher reddenings would have been mostly inaccessible to IUE, and at that time there were few objects with known high values of R_{5495} . For the three wavelength ranges the following functional forms were used:

- **UV:** An adaptation of the Fitzpatrick & Massa (1988) functional form (see below).
- **Optical:** A 7th degree polynomial in $x \equiv 1/\lambda$ to interpolate between the central wavelengths of the Johnson photometric bands.
- **IR:** A power law $A(\lambda) \propto \lambda^{-\alpha}$ with a fixed value of $\alpha = 1.61$ from Rieke & Lebofsky (1985).

⁴As proof of the importance of the paper, it is currently the 11th most cited paper on ADS, with a citation count approaching 10 000 at the time of the writing of this contribution.

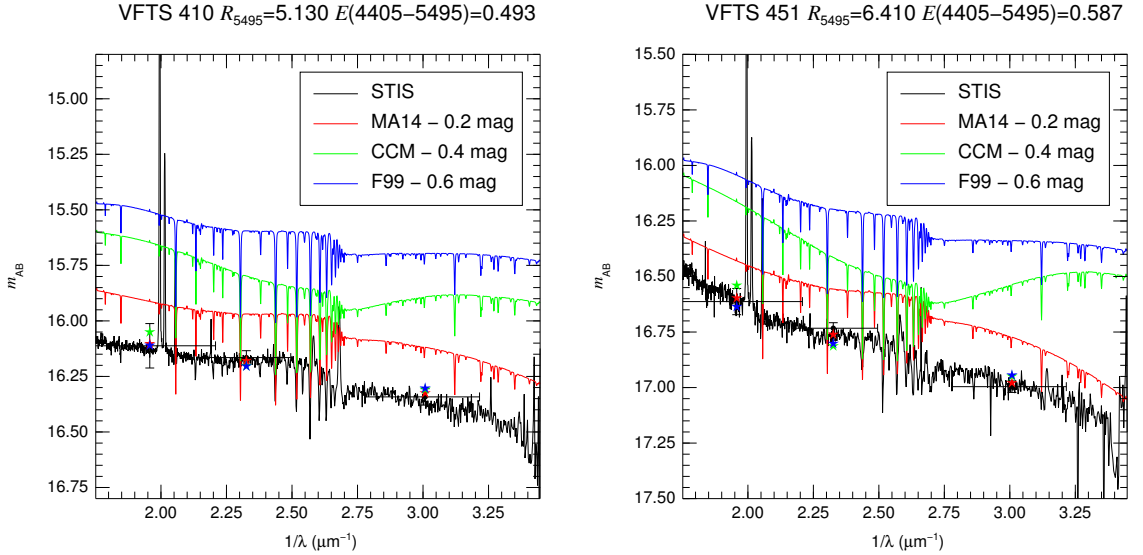


Figure 10: Comparison between the STIS spectrophotometry for two 30 Dor stars in the MA14 sample and the fits using the three families of extinction laws discussed in this contribution. Note how the use of splines in F99 and MA14 allow them to follow the approximate shape of the spectrophotometry while the seventh degree polynomial used by CCM introduces unphysical oscillations in wavelength.

A decade later, Fitzpatrick (1999) or F99 produced another family of extinction laws. His sample was larger than that of CCM but with a similar sampling⁵ in terms of $E(B - V)$, as the paper is also UV-centric. The main modification with respect to CCM is the use of splines instead of a seventh degree polynomial to interpolate between filter central wavelengths and, in that way, avoid unphysical oscillations in wavelength (Fig. 10). The spline interpolation is extended into the IR and, as a result, the functional form does not follow a power law there. Instead, the slope is flatter at wavelengths longer than the H band and steeper at shorter wavelengths (Fig. 11).

A third family of extinction laws was derived by Maíz Apellániz et al. (2014) or MA14 using a sample of 85 OB stars in 30 Dor observed with

⁵Some of the details of the analysis are hard to follow in that paper, as the sample is not presented in detail but is a modification of that of Fitzpatrick & Massa (1990), their R_V values are not given, and the notation confuses monochromatic and band-integrated quantities.

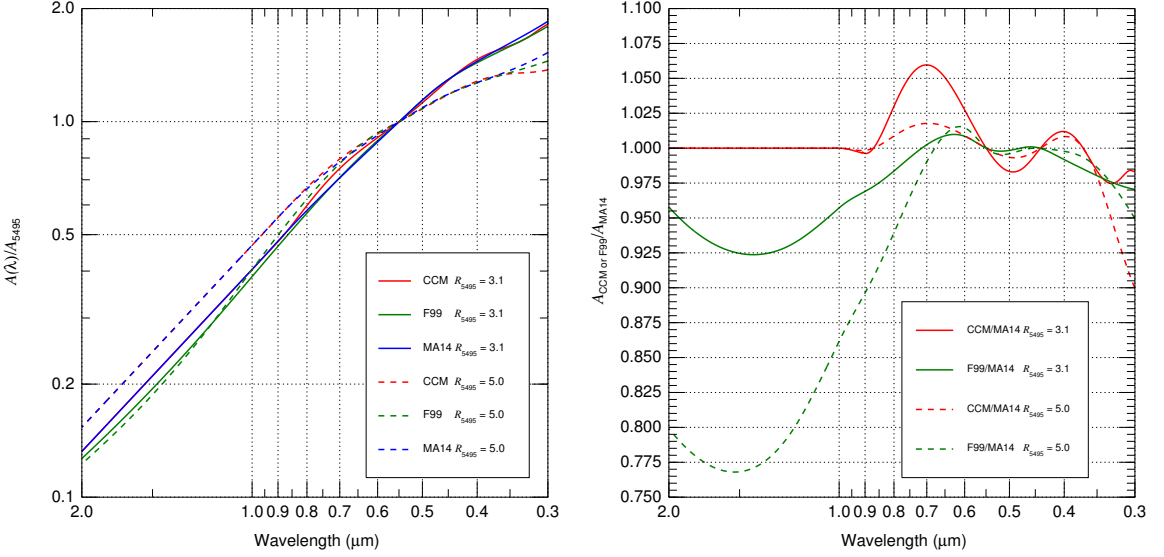


Figure 11: Comparison between the CCM, F99, and MA14 families of extinction laws for two values of R_{5495} , 3.0 and 5.1. The left panel shows the extinction laws normalized to the value at 5495 \AA . The right panel shows the ratio of the CCM and F99 laws to the MA14 one of the same R_{5495} . Note that the CCM and MA14 laws are identical in the IR for a given R_{5495} .

HST/WFC3 *UBVI* optical and ground-based *JHK* photometry. The advantages of HST/WFC3 photometry are its better calibration and spatial resolution, which leads to a reduction in the systematic effects present in Johnson photometry and allows for the detection of possible companions. The covered range in $E(4405 - 5495)$ was smaller than those of CCM or F99 (an effect offset by the better photometric calibration) but with a better sampling in R_{5495} . As opposed to the two previous families, the TLUSTY models used for CHORIZOS were the source for unextinguished SEDs instead of real standard stars.

The idea behind MA14 was to combine the best of both worlds from CCM and F99: the proven behavior of the first as a function of R_{5495} with the use of splines in the optical from the second to eliminate the unphysical oscillations in wavelength. To that purpose, MA14 started with the CCM family, maintained the IR behavior of Rieke & Lebofsky (1985), and substituted the optical part with a spline equivalent. Then, the photometric

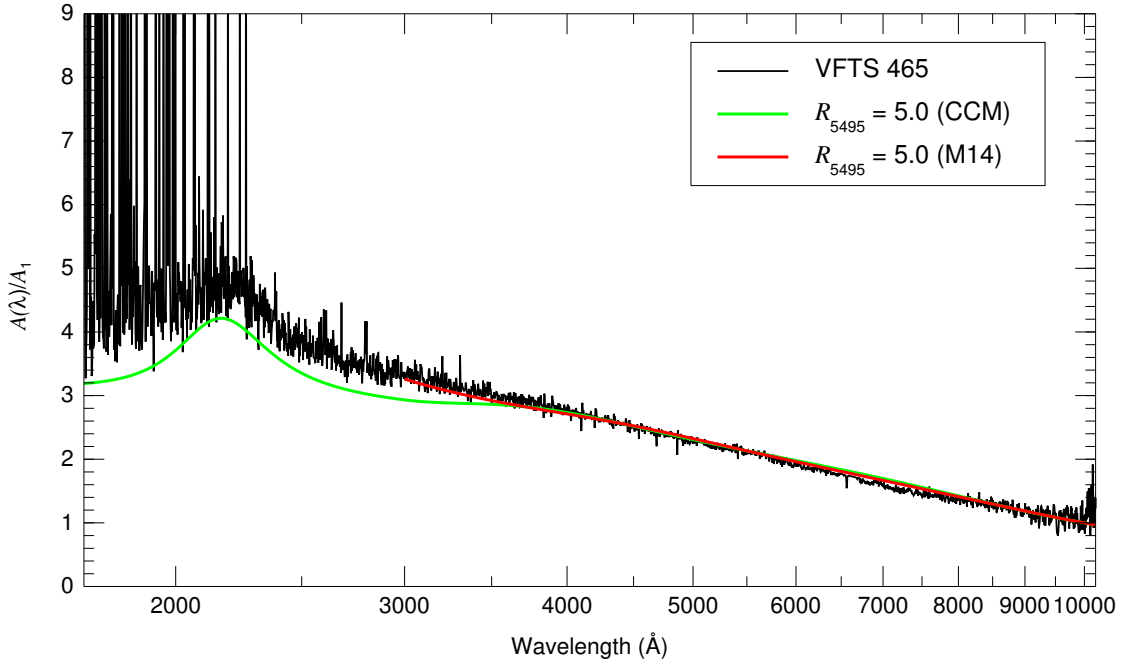


Figure 12: 30 Dor star observed with HST/STIS spectrophotometry and their corresponding SED fits from the photometry in MA14 using the CCM and the new families in that paper. Both fits are very good in the optical but in the U band the new laws are significantly better, leading to the possibility that some of the differences in the UV slope arise not from a difference in extinction laws between the Milky Way and 30 Dor but due to a bad stitching between the optical and UV regimes in CCM. I have not removed the effects of narrow ISM lines in the NUV, the mismatch in the profiles of stellar lines in the optical, or the noise in the FUV and around $1 \mu\text{m}$.

residuals were studied to discover that the CCM laws were underestimating extinction in the U band (the same is true for F99) and corrected for that effect (Fig. 12). The shortcomings of the family are that it does not include the UV; that the IR slope is assumed and not determined (something difficult to do for the range of extinctions of the sample); and that, being derived from 30 Dor data, its validity for Galactic sightlines was unproven at the time of the writing of the paper (but see below).

There are other published families of extinction laws but I restrict the analysis to these three, as the first two are the ones most often used in

the literature and the third one is used for the comparison in the next subsection. In Fig. 11 I plot a comparison between the three families, which is a graphical summary of some of the points I have made in this subsection.

- The CCM and MA14 families follow a power law with $\alpha = 1.61$ and are identical in the NIR, so they are shown as superimposed straight lines in the left panel and a value of 1.0 in the right one for that range. The F99 families, on the other hand are not power laws in the NIR and they predict less extinction there for the same amount of optical extinction. The differences between CCM/MA14 and F99 in the NIR increase with R_{5495} .
- The differences between the three families are smaller in the optical than those between CCM/MA14 and F99 in the NIR.
- The CCM family has an oscillatory behavior in the optical range due to the use of a seventh degree polynomial in $1/\lambda$ for interpolation.
- Both the CCM and F99 families predict a lower extinction in the U band for the same amount of extinction in the V band.

4.2. THE OPTICAL/NIR

Having presented the characteristics of the three families of extinction laws, the outstanding question is: which one of the three is a better approximation to reality? The answer was provided by Maíz Apellániz & Barbá (2018), whose work on the distribution of $E(4405 - 5495)$ vs. R_{5495} for 562 O-type Galactic stars was presented in the previous section. That paper also processed their Johnson+2MASS+*Gaia* photometry (with Tycho-2 and/or Strömgren included when available) through CHORIZOS using the three families. The resulting reduced χ^2 distributions are shown in Fig. 13

- As seen in the bottom right panel, the best results are clearly obtained with the MA14 family. The observed reduced χ^2 distribution follows the expected one closely, with no target having a value over 4. On the other hand, both the CCM and F99 families have extended tails into high reduced χ^2 values that indicate that they cannot provide accurate fits for some of the stars in the sample, with four of the five the worst outliers coming from F99. **The family of extinction laws**

EXTINCTION, THE ELEPHANT IN THE ROOM

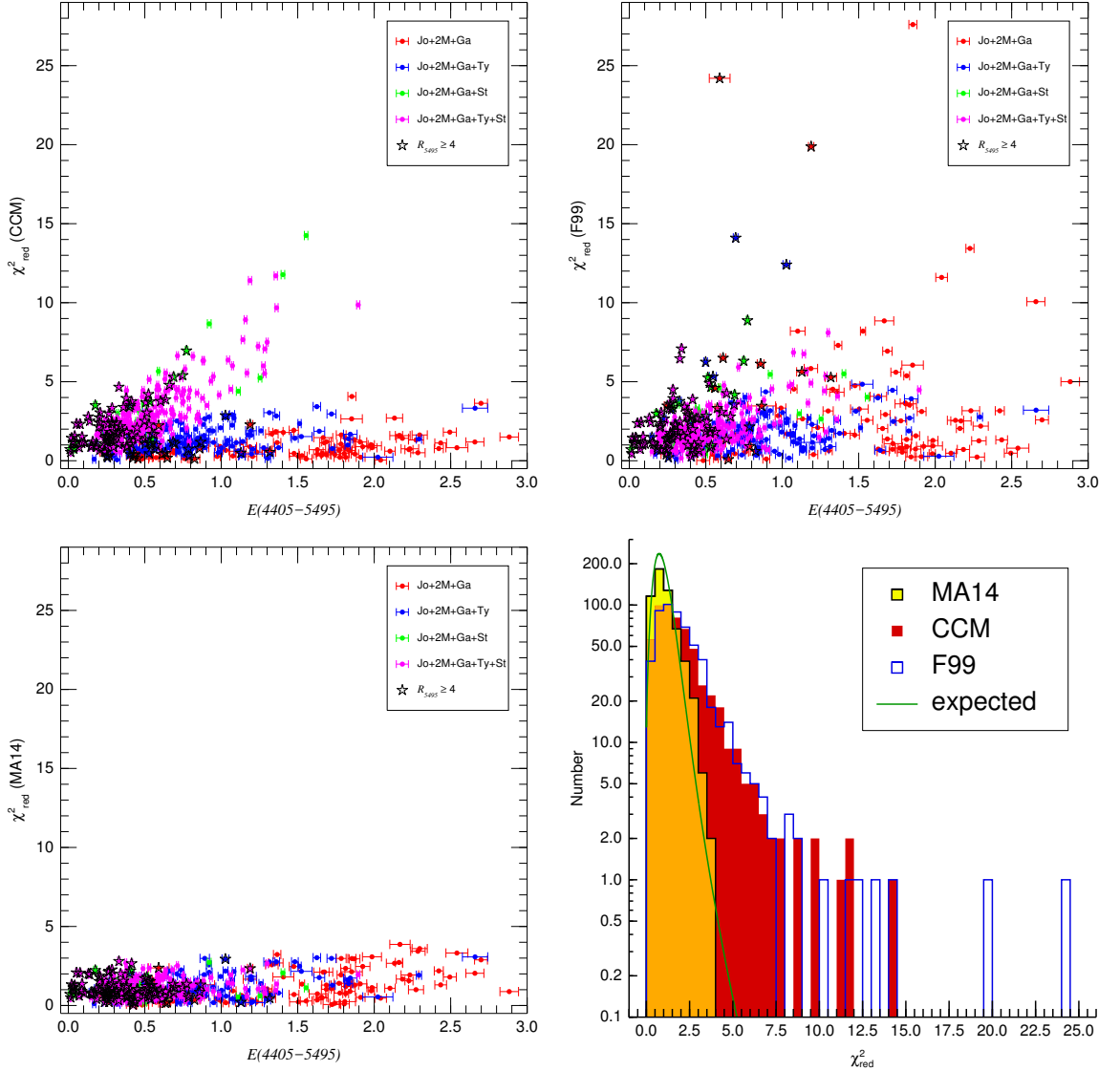


Figure 13: Reduced χ^2 as a function of $E(4405 - 5495)$ using the CCM (top left), F99 (top right), and MA14 (bottom left) families of extinction laws for the CHORIZOS runs of the Galactic O-star sample of Maíz Apellániz & Barbá (2018). (bottom right) Reduced χ^2 histograms for the first three plots and expected distribution.

of Maíz Apellániz et al. (2014) provides the best description of Galactic optical extinction for $E(4405 - 5495) < 3.0$ available to date.

- For CCM, the worst results are those where Strömgren photometry is included. This is expected given the seventh degree polynomial used for that family. The tight correlation shown between the reduced χ^2 and $E(4405 - 5495)$ in the top left panel for those targets is a telltale sign that the effect is caused by extinction. Other than that, CCM provides a reasonable behavior in the sampled range.
- For F99, the worst results are those for high values of R_{5495} , marked with stars in the top right panel. However, there is also a significant trend of increasing reduced χ^2 with $E(4405 - 5495)$ for targets with near-canonical values of R_{5495} .
- I point out once more that the three families of extinction laws were developed using stars that are essentially in the leftmost one-third of the $E(4405 - 5495)$ range of the CCM/F99/MA14 panels of Fig. 13. For stars in the remaining two-thirds we are extrapolating the behavior from there.

The analysis of Maíz Apellániz & Barbá (2018) was extended by Maíz Apellániz et al. (2021b) to include more stars, especially with large values of extinction (reaching $E(4405 - 5495) = 3.5$). They found that even with the MA14 family, some stars have reduced χ^2 values larger than 4. This means that the extrapolation from low extinctions is already failing and that an improved family is needed. Below I address how new data could be used to achieve that.

4.3. THE UV

Fitzpatrick & Massa (1988) parameterized UV extinction as a function of $x \equiv 1/\lambda$ (in μm^{-1}) as the sum of three components: a linear term, a Drude function (for the 2175 Å bump) and a far-UV rise. The formula in that paper is:

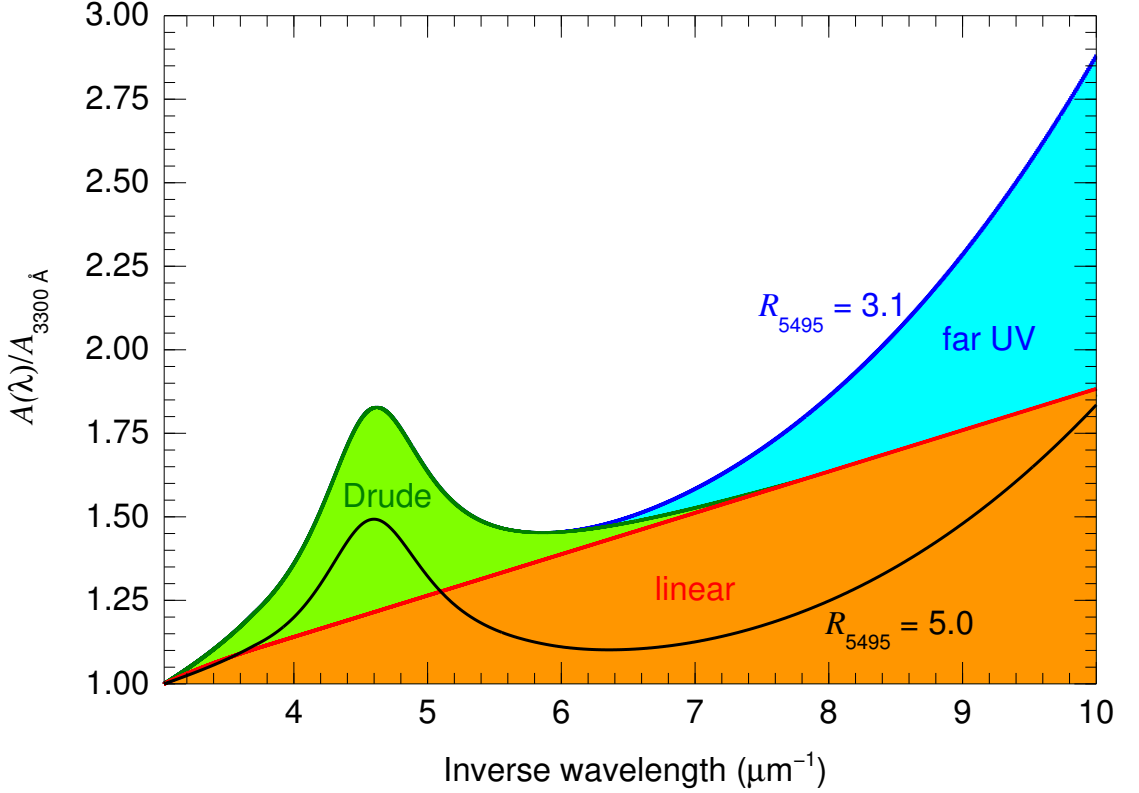


Figure 14: F99 UV extinction for R_{5495} of 3.1 and 5.0. The $R_{5495} = 3.1$ case has been decomposed into its three components (linear, Drude profile, and far-UV rise).

$$\frac{A(\lambda) - A_V}{E(B - V)} = c_1 + c_2x + c_3D(x; \gamma, x_0) + c_4F(x), \quad (9)$$

$$D(x; \gamma, x_0) = \frac{x^2}{(x^2 - x_0^2)^2 + x^2\gamma^2}, \quad (10)$$

$$F(x) = \begin{cases} 0.5392(x - 5.9)^2 + 0.05644(x - 5.9)^3 & \text{for } x \geq 5.9 \\ 0 & \text{for } x < 5.9 \end{cases} \cdot \quad (11)$$

As I have previously mentioned, such formulae should not be expressed in terms of band-integrated quantities [A_V or $E(B - V)$] and in a consistent

implementation they should be substituted by their monochromatic equivalents. In Fig. 14 I represent the UV extinction as implemented by F99 using those formulae but renormalized to 1.0 at the beginning of the UV range and based on R_{5495} . CCM used a similar but slightly different parameterization in the UV but the overall characteristics are the same. Both CCM and F99 used a number of sightliness to derive relationships that express the six parameters in Eqns. 9-11 (c_1 , c_2 , c_3 , c_4 , x_0 , and γ) as a function of R_{5495} (or its equivalent). When combined with the optical/IR results, the final outcome in each paper is a single-parameter family that covers the three wavelength ranges.

The main effect of increasing R_{5495} in either the CCM or F99 families is to make the UV slope flatter (for extreme R_{5495} values, the linear component can actually be negative). For the LMC and SMC (see references at the beginning of the previous section) the most important effect is the reduction in c_3 , the intensity of the Drude profile.

As opposed to the results in CCM and F99, the analysis of Fitzpatrick & Massa (2007) found a very different result: with the exception of few cases with extreme values of R_{5495} , the UV and IR portions of the Galactic extinction curves are not correlated with each other. In other words, it is not possible to derive a single-parameter (e.g. R_{5495}) family of extinction laws for the three wavelength ranges, as UV and IR extinctions behave independently. In a subsequent paper, Fitzpatrick & Massa (2009) attempted to derive a two-parameter family of extinction laws but, as shown in Appendix E of Maíz Apellániz & Barbá (2018), the analysis was flawed because they inadvertently made one parameter a function of the other one. In a recent paper involving those authors (Gordon et al. 2023) they derive a new family of extinction laws based on a single parameter for the UV/optical/IR ranges and only reference Fitzpatrick & Massa (2007) in passing.

4.4. THE IR

As already mentioned, Rieke & Lebofsky (1985) approximated the NIR extinction law with a power law:

$$A(\lambda) = A_1 \lambda^{-\alpha}, \quad (12)$$

where A_1 is the extinction at 1 μm , α is the power-law exponent, and λ is expressed in μm . Rieke & Lebofsky (1985) obtained $\alpha = 1.61$, which is

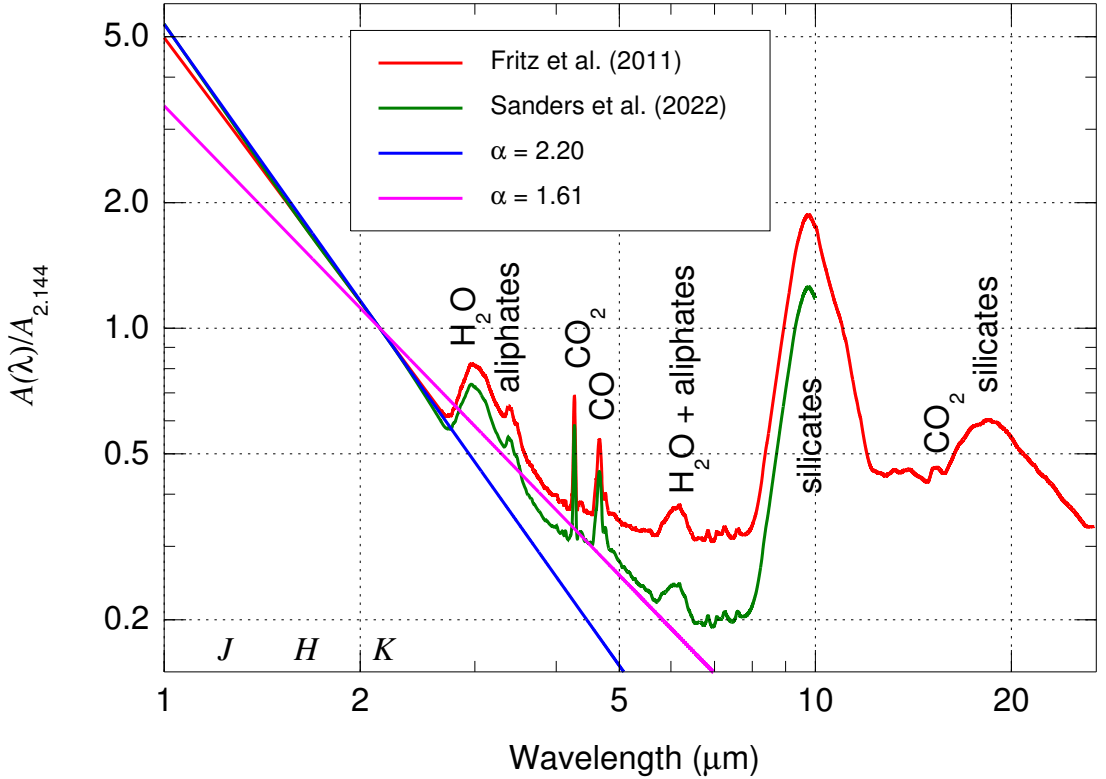


Figure 15: IR extinction laws normalized to $2.144 \mu\text{m}$ from Fritz et al. (2011) and Sanders et al. (2022). As a comparison, two power laws with α of 2.20 and 1.61 are also shown. The location of the *JHK* bands and the identification of the main absorption features are printed.

the value that CCM and MA14 used. On the other hand, most results of the last 15 years (Stead & Hoare 2009; Fritz et al. 2011; Schultheis et al. 2015; Damineli et al. 2016; Alonso-García et al. 2017; Nogueras-Lara et al. 2018; Maíz Apellániz et al. 2020; Sanders et al. 2022) have obtained significantly higher values of α between 2.11 and 2.47, with most in the range 2.2 ± 0.1 . One of the reasons for the discrepancy with the Rieke & Lebofsky (1985) result is that the latter inadvertently included Cyg OB2-12 in their sample, a B-type variable hypergiant with a strong wind and a significant IR excess (Salas et al. 2015; Nazé et al. 2019) which flattens the

derived extinction law if not corrected for. Also, most recent papers show little sightline-dependence variability either with direction or amount of extinction (Stead & Hoare 2009; Wang & Jiang 2014; Schultheis et al. 2015; Nogueras-Lara et al. 2018; Maíz Apellániz et al. 2020) and a progressive flattening of the slope as we move from the JH bands to the K band and beyond (Fritz et al. 2011; Nogueras-Lara et al. 2019; Sanders et al. 2022), indicating that IR extinction cannot be approximated by a power law over the whole range (Hosek et al. 2018).

There are no known strong absorption features in the JHK bands (or NIR) but the situation changes in the MIR, with significant absorption features arising from H_2O , CO , CO_2 , aliphates, and silicates (Fritz et al. 2011; Sanders et al. 2022; Declair et al. 2022), see Fig. 15. The flattening detected by some authors between the JH and HK bands becomes more significant in the 3-8 μm region (once the absorption features are removed) with values of $\alpha \sim 1.5$ or even lower.

One apparently discrepant voice is that of Declair et al. (2022) who measure $\alpha = 1.7$ using relatively low-extinction OB stars. The difference is not due to the nature of the targets (as OB stars inhabit, in principle, different typical environments than late-type giants, see Maíz Apellániz & Barbá 2018 for the effects on extinction), as Daminieli et al. (2016) measured a value of 2.13 ± 0.08 also using OB stars (albeit more extinguished). Instead, I suspect the difference is caused by a combination of two effects:

- The low extinction of their targets (compared to most other similar studies) makes their results more subject to systematic errors. Indeed, the values they obtain for α vary between 1.36 and 2.20, a range much larger than what is seen in other studies. Also, their Fig. 5 reveals that the power-law fit is not a good approximation for the data of some of their wavelength regions and stars.
- Their wavelength range is large, covering 0.8-5.5 μm for some of their stars, as opposed to the narrower JHK range of most studies above. We have already seen that the extinction law flattens for wavelengths longer than the K band and the same is true in the 0.8-1.0 μm region (Fig. 11). Therefore, an average α in the 0.8-5.5 μm range is likely to be lower than its equivalent for the JHK bands.

5. The future

Extinction makes stars look faint but the future for extinction studies looks bright. The most significant improvement will be spectrophotometry substituting the role of photometry, thus dissipating the doubts over the functional form of the extinction law and allowing for the detection of possible structures at intermediate wavelength scales, such as the already known 7700 Å bump. For the case of the Magellanic Clouds (and, later on, for other galaxies) there is plenty of room to significantly increase the number of studied sightlines. Regarding spectrophotometry, in the optical *Gaia* XP is likely to play the major role thanks to its large sample size and dynamic range and despite its poor spectral resolution. That may be complemented with HST/STIS data for a few sightlines, especially if the mission does not end soon. In the IR there is still ISO and Spitzer archival data to be fully analyzed but new data may come from ground-based observations and from JWST, though in the latter case I am somewhat pessimistic that panels will assign much time to bright objects (as many extinguished stars are in the IR). In the UV HST is likely to still be the main contributor in the short term with projects such as ULLYSES (Roman-Duval et al. 2023) until new missions are launched.

Another line that should be explored is the improvement in calibrations provided by *Gaia* (spectro)photometry applied to ground-based photometric surveys. That will allow detailed extinction studies to complement *Gaia* with narrow and intermediate bands. An example of that type of study is GALANTE (Maíz Apellániz et al. 2021a)

Extinction should be understood as the effect of ISM material on astronomical light sources, independently of whether the material is “generic” dust extinguishing the continuum or is in lines/bands assigned to a known or suspected material. This is already done in the NIR (Fig. 15) and in the UV with the 2175 Å band (long suspected to originate in graphite). Therefore, the extinction law should eventually incorporate atomic and molecular lines, which would introduce further complications. First, is that different environments in terms of composition, depletion, and ionization state will contribute to different degrees to extinction, thus necessitating multi-parameter families. Second, some lines like the optical Na I and Ca II doublets easily saturate near the Galactic plane and their measured EWs depend not only on the column density but on the temperature and kinematics along the

sightline. However, even approximately incorporating them into an extinction line would provide us information on the conditions associated with different components of the ISM, such as the excess Ca II absorption associated with high-velocity clouds (Routly & Spitzer 1951, 1952).

The final components that should be added to the extinction law are DIBs, ISM bands discovered a century ago (Heger 1922; Merrill 1934) but of still uncertain nature save a few ascribed to fullerenes (Foing & Ehrenfreund 1994). It is known that there are different types of sightlines (Krełowski et al. 1997; Cami et al. 1997), named σ and ζ after the prototypes σ Sco and ζ Oph, that sample different regimes of the ISM based on the exposure to UV radiation. The DIB EWs are well correlated with $E(4405 - 5495)$ and the sightline type is weakly correlated with R_{5495} (Maíz Apellániz 2015), so there is hope that a multi-parameter extinction law could incorporate a significant part of the DIB behavior.

Acknowledgements

I would like to thank the LOC for organizing a nice meeting in such a beautiful location. I acknowledge support from the Spanish Government Ministerio de Ciencia, Innovación y Universidades, Agencia Estatal de Investigación (10.13039/501100011033), and FEDER/UE through grant PGC2018-095049-B-C22 and grant PID2022-136640NB-C22 from the Consejo Superior de Investigaciones Científicas (CSIC) through grant 2022-AEP 005.

References

- Alonso-García, J., Minniti, D., Catelan, M., et al. 2017, *ApJL*, 849, L13
Baade, W. & Minkowski, R. 1937, *ApJ*, 86, 123
Berlanas, S. R., Maíz Apellániz, J., Herrero, A., et al. 2023, *A&A*, 671, A20
Blanco, V. M. 1956, *ApJ*, 123, 64
Blanco, V. M. 1957, *ApJ*, 125, 209
Bohlin, R. C. 2007, in *ASP Conf. Series*, Vol. 364, *The Future of Photometric, Spectrophotometric and Polarimetric Standardization*, ed. C. Sterken, 315–331
Bohlin, R. C. 2014, *AJ*, 147, 127
Bohlin, R. C. & Gilliland, R. L. 2004, *AJ*, 127, 3508
Brown, A. G. A., Vallenari, A., Prusti, T., et al. 2016, *A&A*, 595, A2
Cami, J., Sonnentrucker, P., Ehrenfreund, P., & Foing, B. H. 1997, *A&A*, 326, 822
Cardelli, J. A., Clayton, G. C., & Mathis, J. S. 1989, *ApJ*, 345, 245
Cardelli, J. A. & Savage, B. D. 1988, *ApJ*, 325, 864
Carrasco, J. M., Weiler, M., Jordi, C., et al. 2021, *A&A*, 652, A86
Clayton, G. C. & Martin, P. G. 1985, *ApJ*, 288, 558
Creevey, O. L., Sordo, R., Pailer, F., et al. 2023, *A&A*, 674, A26
Damineli, A., Almeida, L. A., Blum, R. D., et al. 2016, *MNRAS*, 463, 2653
Declair, M., Gordon, K. D., Andrews, J. E., et al. 2022, *ApJ*, 930, 15
Draine, B. T. 2011, *Physics of the Interstellar and Intergalactic Medium* (Princeton University Press)
Drew, J. E., Greimel, R., Irwin, M. J., et al. 2005, *MNRAS*, 362, 753
Finkbeiner, D. P. 2003, *ApJS*, 146, 407
Fitzpatrick, E. L. 1985, *ApJ*, 299, 219
Fitzpatrick, E. L. 1986, *AJ*, 92, 1068
Fitzpatrick, E. L. 1999, *PASP*, 111, 63
Fitzpatrick, E. L. & Massa, D. 1988, *ApJ*, 328, 734
Fitzpatrick, E. L. & Massa, D. 1990, *ApJS*, 72, 163
Fitzpatrick, E. L. & Massa, D. 2005, *AJ*, 130, 1127
Fitzpatrick, E. L. & Massa, D. 2007, *ApJ*, 663, 320
Fitzpatrick, E. L. & Massa, D. 2009, *ApJ*, 699, 1209
Fitzpatrick, E. L. & Savage, B. D. 1984, *ApJ*, 279, 578
Foing, B. H. & Ehrenfreund, P. 1994, *Nature*, 369, 296
Fritz, T. K., Gillessen, S., Dodds-Eden, K., et al. 2011, *ApJ*, 737, 73
Gordon, K. D. & Clayton, G. C. 1998, *ApJ*, 500, 816
Gordon, K. D., Clayton, G. C., Declair, M., et al. 2023, *ApJ*, 950, 86
Guhathakurta, P. & Draine, B. T. 1989, *ApJ*, 345, 230

EXTINCTION, THE ELEPHANT IN THE ROOM

- Hecht, J., Helfer, H. L., Wolf, J., Pipher, J. L., & Donn, B. 1982, *ApJL*, 263, L39
- Heger, M. L. 1922, *Lick Observatory Bulletin*, 10, 146
- Hiltner, W. A. & Johnson, H. L. 1956, *ApJ*, 124, 367
- Hosek, Jr., M. W., Lu, J. R., Anderson, J., et al. 2018, *ApJ*, 855, 13
- Howarth, I. D. 1983, *MNRAS*, 203, 301
- Johnson, H. L. & Morgan, W. W. 1953, *ApJ*, 117, 313
- Jones, A. P. 2004, in *Astronomical Society of the Pacific Conference Series*, Vol. 309, *Astrophysics of Dust*, ed. A. N. Witt, G. C. Clayton, & B. T. Draine, 347–368
- Krelowski, J., Schmidt, M., & Snow, T. P. 1997, *PASP*, 109, 1135
- Laidler, V. et al. 2005, *Synphot User’s Guide v5.0 (STScI: Baltimore)*
- Lanz, T. & Hubeny, I. 2003, *ApJS*, 146, 417
- Lanz, T. & Hubeny, I. 2007, *ApJS*, 169, 83
- Lequeux, J., Maurice, E., Prevot-Burnichon, M. L., Prevot, L., & Rocca-Volmerange, B. 1982, *A&A*, 113, L15
- Maíz Apellániz, J. 2004, *PASP*, 116, 859
- Maíz Apellániz, J. 2005, *PASP*, 117, 615
- Maíz Apellániz, J. 2006, *AJ*, 131, 1184
- Maíz Apellániz, J. 2007, in *ASP Conf. Series*, Vol. 364, *The Future of Photometric, Spectrophotometric and Polarimetric Standardization*, ed. C. Sterken, 227–236
- Maíz Apellániz, J. 2013a, in *Highlights of Spanish Astrophysics VII*, 583–589
- Maíz Apellániz, J. 2013b, in *Highlights of Spanish Astrophysics VII*, 657–657
- Maíz Apellániz, J. 2015, *MmSAI*, 86, 553
- Maíz Apellániz, J., Alfaro, E. J., Barbá, R. H., et al. 2021a, *MNRAS*, 506, 3138
- Maíz Apellániz, J. & Barbá, R. H. 2018, *A&A*, 613, A9
- Maíz Apellániz, J., Barbá, R. H., Caballero, J. A., Bohlin, R. C., & Fariña, C. 2021b, *MNRAS*, 501, 2487
- Maíz Apellániz, J., Evans, C. J., Barbá, R. H., et al. 2014, *A&A*, 564, A63 (MA14)
- Maíz Apellániz, J., Holgado, G., Pantaleoni González, M., & Caballero, J. A. 2023, *A&A*, 677, A137
- Maíz Apellániz, J., Pantaleoni González, M., Barbá, R. H., García-Lario, P., & Noguerras-Lara, F. 2020, *MNRAS*, 496, 4951
- Maíz Apellániz, J. & Rubio, M. 2012, *A&A*, 541, A54
- Maíz Apellániz, J. & Weiler, M. 2018, *A&A*, 619, A180
- Massa, D., Savage, B. D., & Fitzpatrick, E. L. 1983, *ApJ*, 266, 662
- Merrill, P. W. 1934, *PASP*, 46, 206
- Morgan, W. W. 1944, *AJ*, 51, 21
- Munari, U., Sordo, R., Castelli, F., & Zwitter, T. 2005, *A&A*, 442, 1127

EXTINCTION, THE ELEPHANT IN THE ROOM

- Nazé, Y., Rauw, G., Czesla, S., Mahy, L., & Campos, F. 2019, *A&A*, 627, A99
- Nogueras-Lara, F., Gallego-Calvente, A. T., Dong, H., et al. 2018, *A&A*, 610, A83
- Nogueras-Lara, F., Schödel, R., Najarro, F., et al. 2019, *A&A*, 630, L3
- Nogueras-Lara, F., Schödel, R., & Neumayer, N. 2021, *A&A*, 653, A133
- Prévot, M. L., Lequeux, J., Maurice, E., Prévot, L., & Rocca-Volmerange, B. 1984, *A&A*, 132, 389
- Rieke, G. H. & Lebofsky, M. J. 1985, *ApJ*, 288, 618
- Rocca-Volmerange, B., Prevot, L., Ferlet, R., Lequeux, J., & Prevot-Burnichon, M. L. 1981, *A&A*, 99, L5
- Roman-Duval, J., Taylor, J., Fullerton, A., Fischer, W., & Plesha, R. 2023, in *American Astronomical Society Meeting Abstracts*, Vol. 55, *American Astronomical Society Meeting Abstracts*, 223.02
- Routly, P. M. & Spitzer, Lyman, J. 1952, *ApJ*, 115, 227
- Routly, P. M. & Spitzer, Jr., L. 1951, *AJ*, 56, 138
- Salas, J., Maíz Apellániz, J., & Barbá, R. H. 2015, in *HSA* 8, 615–615
- Sanders, J. L., Smith, L., González-Fernández, C., Lucas, P., & Minniti, D. 2022, *MNRAS*, 514, 2407
- Schultheis, M., Kordopatis, G., Recio-Blanco, A., et al. 2015, *A&A*, 577, A77
- Seaton, M. J. 1979, *MNRAS*, 187, 73P
- Skrutskie, M. F., Cutri, R. M., Stiening, R., et al. 2006, *AJ*, 131, 1163
- Stead, J. J. & Hoare, M. G. 2009, *MNRAS*, 400, 731
- Stebbins, J. & Whitford, A. E. 1943, *ApJ*, 98, 20
- Trumpler, R. J. 1934, *PASP*, 46, 208
- Wang, S. & Chen, X. 2019, *ApJ*, 877, 116
- Wang, S. & Jiang, B. W. 2014, *ApJL*, 788, L12
- York, D. G., Adelman, J., Anderson, John E., J., et al. 2000, *AJ*, 120, 1579